

Frequency-weighted \mathcal{H}_2 -optimal model order reduction via oblique projection

Umair Zulfiqar^a, Victor Sreeram^a, Mian Ilyas Ahmad^b, and Xin Du^{c,d,e}

^aSchool of Electrical, Electronics and Computer Engineering, The University of Western Australia (UWA), Perth, Australia; ^bResearch Centre for Modelling and Simulation, National University of Sciences and Technology (NUST), Islamabad, Pakistan; ^cSchool of Mechatronic Engineering and Automation, and Shanghai Key Laboratory of Power Station Automation Technology, Shanghai University, Shanghai, China; ^dKey Laboratory of Knowledge Automation for Industrial Processes, Ministry of Education, Beijing, China; ^eKey Laboratory of Modern Power System Simulation and Control & Renewable Energy Technology, Ministry of Education (Northeast Electric Power University), Jilin, China

ARTICLE HISTORY

Compiled February 28, 2025

ABSTRACT

In projection-based model order reduction, a reduced-order approximation of the original full-order system is obtained by projecting it onto a reduced subspace that contains its dominant characteristics. The problem of frequency-weighted \mathcal{H}_2 -optimal model order reduction is to construct a local optimum in terms of the \mathcal{H}_2 -norm of the weighted error transfer function. In this paper, a projection-based model order reduction algorithm is proposed that constructs reduced-order models that nearly satisfy the first-order optimality conditions for the frequency-weighted \mathcal{H}_2 -optimal model order reduction problem. It is shown that as the order of the reduced model is increased, the deviation in the satisfaction of the optimality conditions reduces further. Numerical methods are also discussed that improve the computational efficiency of the proposed algorithm. Three numerical examples are presented to demonstrate the efficacy of the proposed algorithm.

KEYWORDS

\mathcal{H}_2 -optimal; frequency-weighted; model order reduction; nearly optimal; projection; suboptimal

1. Introduction

The complexity of the modern-day dynamic systems has been growing rapidly with each passing day. The direct simulation of the high-order mathematical models that describe large-scale dynamic systems requires a huge amount of computational resources, which are limited due to high economic cost of the memory resources. To address this issue, model order reduction (MOR) algorithms are used to obtain reduced-order models (ROMs) that are computationally cheaper to simulate, and they closely mimic the original high-order models. The reduced models can then be used as a surrogate in the design and analysis with tolerable approximation error (Antoulas, 2005; Benner et al., 2017, 2005).

Projection-based MOR is a large family of algorithms wherein the original high-order model is projected onto a reduced subspace that contains its dominant characteristics. The sense of dominance determines the specific type of MOR procedure. Most of the projection-based MOR methods require solutions of some Lyapunov or Sylvester equations to construct the required ROM (Antoulas, 2005). During the last two decades, several computationally efficient low-rank methods for the solution of Lyapunov and Sylvester equations have been proposed, cf. (Ahmad et al., 2010; Gugercin et al., 2003; Li and White, 2002; Penzl, 1999a). By using these methods for solving large-scale linear matrix equations, a ROM of the original large-scale model can be constructed within the admissible time for most of the projection-based MOR algorithms.

Balanced truncation (BT) (Moore, 1981) is one of the most important projection-based MOR method, which is famous for its stability preservation, high fidelity, and *a priori* error bound expression (Enns, 1984). In BT, the original model is projected onto the dominant eigenspace of the product of controllability and observability gramians. The computation of controllability and observability gramians requires the solution of two high-order Lyapunov equations, which is a computationally expensive task in large-scale settings. However, their low-rank solutions can be obtained cheaply, which extends the applicability of BT to large-scale systems (Wolf et al., 2013). In some situations like reduced-order controller design, it is required that the MOR procedure has a low frequency-weighted approximation error. This necessitates the inclusion of frequency-weights in the MOR algorithm. In (Enns, 1984), BT is generalized to incorporate frequency weights in the approximation criterion, which leads to frequency-weighted BT (FWBT). The original model in FWBT is projected onto the dominant eigenspace of the product of frequency-weighted controllability and frequency-weighted observability gramians. Again, the applicability of FWBT can be extended to large-scale systems by using low-rank solutions of linear matrix equations (Ahmad et al., 2010). Several modifications and extensions to FWBT are reported in the literature to ensure additional properties like stability (Wang et al., 1999) and passivity (Zulfiqar et al., 2017); see (Ghafoor and Sreeram, 2008; Obinata and Anderson, 2012) for a detailed survey.

Another important class of projection-based MOR techniques is the Krylov subspace-based methods wherein the full-order system is projected onto a low-dimensional subspace spanned by the columns of a matrix constructed so that the projected reduced system achieves moment matching, i.e., the ROM matches some coefficients of the series expansion of the original transfer function at some selected frequency points (Beattie and Gugercin, 2014). Among these methods is the famous iterative rational Krylov algorithm (IRKA) (Gugercin et al., 2008; Van Dooren et al., 2008), which constructs a local optimum for the \mathcal{H}_2 -optimal MOR problem, i.e., the best among all the ROMs with the same modal configuration and size in minimizing the \mathcal{H}_2 -norm of the error transfer function. Unlike the BT method, IRKA (Gugercin et al., 2008; Van Dooren et al., 2008) does not require the solutions of large-scale Lyapunov equations. Thus it is computationally efficient and can handle large-scale systems. IRKA is heuristically generalized to the frequency-weighted scenario in (Anić et al., 2013) and (Zulfiqar and Sreeram, 2018). The algorithms proposed in (Anić et al., 2013) and (Zulfiqar and Sreeram, 2018) ensure less \mathcal{H}_2 -norm of the weighted error transfer function; however, they do not seek to construct local optimum for the frequency-weighted \mathcal{H}_2 -optimal MOR problem.

In (Halevi, 1990), the first-order optimality conditions for the single-sided case of frequency-weighted \mathcal{H}_2 -optimal MOR are derived, and an algorithm based on Lya-

punov and Riccati equations is proposed to satisfy these conditions. This algorithm is numerically tractable only for small-scale systems. The optimality conditions derived in (Halevi, 1990) are shown equivalent to the tangential interpolation conditions in (Breiten et al., 2015), and a Krylov subspace-based iterative algorithm is proposed, which nearly satisfies these conditions. In (Zulfiqar et al., 2019), an iteration-free Krylov subspace-based algorithm is presented, which exactly satisfies a subset of the optimality conditions while guaranteeing the stability of the ROM at the same time.

The first-order optimality conditions for the double-sided case of the frequency-weighted \mathcal{H}_2 -optimal MOR are derived in (Diab et al., 2000; Petersson, 2013; Yan et al., 1997). The algorithms presented to generate the local optimum in (Diab et al., 2000; Huang et al., 2001; Li et al., 1999; Petersson, 2013; Spanos et al., 1990; Yan et al., 1997) are not feasible for large-scale systems due to high computational cost associated with nonlinear optimization. In (Zulfiqar et al., 2019), the frequency-weighted iterative tangential interpolation algorithm (FWITIA) is proposed that ensures less frequency-weighted \mathcal{H}_2 -norm of the error transfer function in the double-side case. However, its connection with the optimality conditions derived in (Petersson, 2013) is not investigated, which has motivated the work in this paper.

In this paper, we consider the double-sided case of the frequency-weighted \mathcal{H}_2 -optimal MOR problem within the projection framework. The main motivation for seeking a projection-based solution is to avoid nonlinear optimization and benefit from the efficient Sylvester equation solver, particularly formulated for the projection-based \mathcal{H}_2 -optimal MOR algorithms, cf. (Benner et al., 2011). We show that the exact satisfaction of the optimality conditions is inherently not possible within the projection framework. However, the optimality conditions can be nearly satisfied, and the deviation in the satisfaction of the optimality condition decays as the order of ROM grows. The conditions for exact satisfaction of the optimality conditions are also discussed. In addition, a projection-based iterative algorithm is proposed that solves the Sylvester equations in each iteration to construct the required ROM. Upon convergence, the ROM nearly satisfies the first-order optimality conditions for the double-sided case of the frequency-weighted \mathcal{H}_2 -optimal MOR problem. Moreover, it is shown that FWITIA also seeks to satisfy the optimality conditions derived in (Petersson, 2013). The efficacy of the proposed algorithm is highlighted by considering one illustrative and two benchmark numerical examples.

The remainder of this paper is organized as follows. The problem under consideration is introduced in Section 2. In addition, FWBT and FWITIA are briefly reviewed. The main contribution of the paper is covered in Sections 3 and 4. The theoretical results proposed in Sections 3 and 4 are numerically verified in Section 5. The paper is concluded in Section 6.

2. Preliminaries

In this section, the frequency-weighted \mathcal{H}_2 -optimal MOR problem is introduced, and two important existing projection-based algorithms are briefly reviewed. The important mathematical notations used throughout the text are given in Table 1.

Table 1.: Mathematical Notations

Notation	Meaning
$[\cdot]^*$	Hermitian
$tr(\cdot)$	Trace
$Ran(\cdot)$	Range
$orth(\cdot)$	Orthogonal basis
\perp	Orthogonal
\supset	Superset
$span_{i=1,\dots,r} \{\cdot\}$	Span of the set of r vectors

2.1. Problem Setting

Let us denote an n^{th} -order stable linear time-invariant system with m inputs and p outputs as $H(s)$, which is represented as

$$H(s) = C(sI - A)^{-1}B + D \quad (1)$$

where $A \in \mathbb{R}^{n \times n}$, $B \in \mathbb{R}^{n \times m}$, $C \in \mathbb{R}^{p \times n}$, and $D \in \mathbb{R}^{p \times m}$. In a large-scale setting, the order n of (1) is high, the matrices (A, B, C) are sparse, $m \ll n$, and $p \ll n$.

Let us denote the r^{th} -order approximation of $H(s)$ as $\tilde{H}(s)$, which can be written as

$$\tilde{H}(s) = \tilde{C}(sI - \tilde{A})^{-1}\tilde{B} + D$$

where $\tilde{A} \in \mathbb{R}^{r \times r}$, $\tilde{B} \in \mathbb{R}^{r \times m}$, $\tilde{C} \in \mathbb{R}^{p \times r}$, and $r \ll n$.

In projection-based MOR, the state-space matrices \tilde{A} , \tilde{B} , and \tilde{C} are obtained as

$$\tilde{A} = \tilde{W}^T A \tilde{V}, \quad \tilde{B} = \tilde{W}^T B, \quad \tilde{C} = C \tilde{V} \quad (2)$$

where $\tilde{V} \in \mathbb{R}^{n \times r}$, $\tilde{W} \in \mathbb{R}^{n \times r}$ and $\tilde{W}^T \tilde{V} = I$. The columns of \tilde{V} span r -dimensional subspace along the kernel of \tilde{W}^T , and $\Pi = \tilde{V} \tilde{W}^T \in \mathbb{R}^{n \times n}$ is an oblique projection onto that subspace.

Let us denote the error transfer function as $E(s)$, which can be written as

$$E(s) = H(s) - \tilde{H}(s) = C_e(sI - A_e)^{-1}B_e$$

in which

$$A_e = \begin{bmatrix} A & 0 \\ 0 & \tilde{A} \end{bmatrix}, \quad B_e = \begin{bmatrix} B \\ \tilde{B} \end{bmatrix}, \quad C_e = [C \quad -\tilde{C}].$$

Let us denote the input and output weights as $W_i(s)$ and $W_o(s)$, respectively, which have the following transfer functions

$$\begin{aligned} W_i(s) &= C_i(sI - A_i)^{-1}B_i + D_i, \\ W_o(s) &= C_o(sI - A_o)^{-1}B_o + D_o \end{aligned}$$

where $A_i \in \mathbb{R}^{n_i \times n_i}$, $B_i \in \mathbb{R}^{n_i \times m}$, $C_i \in \mathbb{R}^{m \times n_i}$, $D_i \in \mathbb{R}^{m \times m}$, $A_o \in \mathbb{R}^{n_o \times n_o}$, $B_o \in \mathbb{R}^{n_o \times p}$, $C_o \in \mathbb{R}^{p \times n_o}$, and $D_o \in \mathbb{R}^{p \times p}$. Also, assume that $W_i(s)$ and $W_o(s)$ are stable.

Further, let us denote the weighted error transfer function as $E_w(s)$, which has the following representation

$$E_w(s) = W_o(s)E(s)W_i(s) = C_w(sI - A_w)^{-1}B_w$$

where

$$\begin{aligned} A_w &= \begin{bmatrix} A & 0 & BC_i & 0 \\ 0 & \tilde{A} & \tilde{B}C_i & 0 \\ 0 & 0 & A_i & 0 \\ B_oC & -B_o\tilde{C} & 0 & A_o \end{bmatrix}, & B_w &= \begin{bmatrix} BD_i \\ \tilde{B}D_i \\ B_i \\ 0 \end{bmatrix}, \\ C_w &= [D_oC \quad -D_o\tilde{C} \quad 0 \quad C_o]. \end{aligned} \quad (3)$$

Let us denote the controllability and observability gramians of the realization (A_w, B_w, C_w) as P_w and Q_w , respectively, which solve the following Lyapunov equations

$$A_w P_w + P_w A_w^T + B_w B_w^T = 0, \quad (4)$$

$$A_w^T Q_w + Q_w A_w + C_w^T C_w = 0. \quad (5)$$

P_w and Q_w can be partitioned according to the structure of the realization in (3) by defining

$$P_w = \begin{bmatrix} P & P_{12} & P_{13} & P_{14} \\ P_{12}^T & \tilde{P} & P_{23} & P_{24} \\ P_{13}^T & P_{23}^T & P_i & P_{34} \\ P_{14}^T & P_{24}^T & P_{34}^T & P_o \end{bmatrix}, \quad Q_w = \begin{bmatrix} Q & Q_{12} & Q_{13} & Q_{14} \\ Q_{12}^T & \tilde{Q} & Q_{23} & Q_{24} \\ Q_{13}^T & Q_{23}^T & Q_i & Q_{34} \\ Q_{14}^T & Q_{24}^T & Q_{34}^T & Q_o \end{bmatrix}.$$

In the frequency-weighted \mathcal{H}_2 -MOR, a ROM $\tilde{H}(s)$ is sought, which ensures that the \mathcal{H}_2 -norm of $E_w(s)$ is small, i.e.,

$$\min_{\substack{\tilde{H}(s) \\ \text{order}=r}} \|E_w(s)\|_{\mathcal{H}_2}.$$

The \mathcal{H}_2 -norm of $E_w(s)$ is the energy of the its impulse response and is related to the controllability and observability gramians of its state-space realization as

$$\begin{aligned} \|E_w(s)\|_{\mathcal{H}_2}^2 &= \text{tr}(C_w P_w C_w^T) = \text{tr}(D_o C P C^T D_o^T + D_o \tilde{C} \tilde{P} \tilde{C}^T D_o^T - 2D_o C P_{12} \tilde{C}^T D_o^T \\ &\quad + C_o P_o C_o^T + 2D_o C P_{14} C_o^T - 2D_o \tilde{C} P_{24} C_o^T) \\ &= \text{tr}(B_w^T Q_w B_w) = \text{tr}(D_i^T B^T Q B D_i + D_i^T \tilde{B}^T \tilde{Q} \tilde{B} D_i + 2D_i^T B^T Q_{12} \tilde{B} D_i \\ &\quad + B_i^T Q_i B_i + 2D_i^T B^T Q_{13} B_i + D_i^T \tilde{B}^T Q_{23} B_i). \end{aligned}$$

$\tilde{H}(s)$ is a local optimum of $\|E_w(s)\|_{\mathcal{H}_2}^2$ if it satisfies the following first-order optimality

conditions

$$\frac{\partial}{\partial \bar{A}} \|E_w(s)\|_{\mathcal{H}_2}^2 = 0 \quad \Rightarrow \quad \bar{X} + X = 0, \quad (6)$$

$$\frac{\partial}{\partial \tilde{B}} \|E_w(s)\|_{\mathcal{H}_2}^2 = 0 \quad \Rightarrow \quad \bar{Y} D_i D_i^T + Y = 0, \quad (7)$$

$$\frac{\partial}{\partial \tilde{C}} \|E_w(s)\|_{\mathcal{H}_2}^2 = 0 \quad \Rightarrow \quad D_o^T D_o \bar{Z} + Z = 0 \quad (8)$$

where

$$\begin{aligned} \bar{X} &= Q_{12}^T P_{12} + \tilde{Q} \tilde{P}, & \bar{Y} &= Q_{12}^T B + \tilde{Q} \tilde{B}, \\ \bar{Z} &= C P_{12} - \tilde{C} \tilde{P}, & X &= Q_{23} P_{23}^T + Q_{24} P_{24}^T, \\ Y &= (Q_{12}^T P_{13} + \tilde{Q} P_{23} + Q_{23} P_i + Q_{24} P_{34}^T) C_i^T + Q_{23} B_i D_i^T, \\ Z &= -B_o^T (Q_{14}^T P_{12} + Q_{24}^T \tilde{P} + Q_{34}^T P_{23}^T + Q_o P_{24}^T) + D_o^T C_o P_{24}^T. \end{aligned}$$

2.2. Frequency-weighted Balanced Truncation

The original system in FWBT is projected onto an r -dimensional dominant eigenspace of PQ . The square roots of the eigenvalues of PQ are called the frequency-weighted Hankel singular values $\hat{\sigma}_i$, and they quantify the energy contribution of the states within the frequency region emphasized by the frequency weights. The $n-r$ states with the least values of $\hat{\sigma}_i$ are truncated. The oblique projection $\Pi = \tilde{V} \tilde{W}^T$ is computed as $\tilde{P} = \tilde{Q} \approx \tilde{W}^T P \tilde{W} = \tilde{V}^T Q \tilde{V} = \text{diag}(\hat{\sigma}_1, \dots, \hat{\sigma}_r)$ where $\hat{\sigma}_1 \geq \dots \hat{\sigma}_r$ are the r largest frequency-weighted Hankel singular values. FWBT does not seek to satisfy the optimality conditions (6)-(8); however, the ROM constructed by FWBT shows high fidelity.

2.3. Frequency-weighted Tangential Interpolation

Here, the goal is to construct a ROM that tends to satisfy the following conditions

$$\frac{\partial}{\partial \tilde{B}} \|W_o(s) E(s)\|_{\mathcal{H}_2}^2 = 2(Q_{12}^T B + \tilde{Q} \tilde{B}) = 0, \quad (9)$$

$$\frac{\partial}{\partial \tilde{C}} \|E(s) W_i(s)\|_{\mathcal{H}_2}^2 = 2(C P_{12} - \tilde{C} \tilde{P}) = 0. \quad (10)$$

Suppose $H(s)$ and $\tilde{H}(s)$ have simple poles. Also, let $\tilde{H}(s)$ has the following pole-residue form

$$\tilde{H}(s) = \sum_{i=1}^r \frac{\tilde{l}_i \tilde{r}_i^T}{s - \tilde{\lambda}_i} + D.$$

Now define $F[H(s)] = C_f(sI - A_f)^{-1}B_f$ and $G[H(s)] = C_g(sI - A_g)^{-1}B_g$ wherein

$$A_f = \begin{bmatrix} A & BC_i \\ 0 & A_i \end{bmatrix}, \quad A_g = \begin{bmatrix} A & 0 \\ B_oC & A_o \end{bmatrix}, \quad (11)$$

$$B_f = \begin{bmatrix} P_{13}C_i^T + BD_iD_i^T \\ P_iC_i^T + B_iD_i^T \end{bmatrix}, \quad B_g = \begin{bmatrix} B \\ B_oD \end{bmatrix}, \quad (12)$$

$$C_f = \begin{bmatrix} C^T \\ C_i^T D_i^T \end{bmatrix}^T, \quad C_g = \begin{bmatrix} Q_{14}B_o + C^T D_o^T D_o \\ Q_oB_o + C_o^T D_o \end{bmatrix}^T. \quad (13)$$

The conditions (9) and (10) can be satisfied if the following tangential interpolation conditions are satisfied, cf., (Zulfiqar et al., 2019),

$$F[H(-\tilde{\lambda}_i)]\tilde{r}_i = \tilde{F}[\tilde{H}(-\tilde{\lambda}_i)]\tilde{r}_i, \quad (14)$$

$$\tilde{l}_i^T G[H(-\tilde{\lambda}_i)] = \tilde{l}_i^T \tilde{G}[\tilde{H}(-\tilde{\lambda}_i)]. \quad (15)$$

The poles $\tilde{\lambda}_i$ and residues $(\tilde{l}_i, \tilde{r}_i)$ of $\tilde{H}(s)$ are not known *a priori*. Thus the interpolation points and tangential directions are initialized arbitrarily, and after every iteration, the interpolation points σ_i are updated as $-\tilde{\lambda}_i$, and the tangential directions (c_i, b_i) are updated as the residues $(\tilde{l}_i, \tilde{r}_i)$. The rational Krylov subspaces that seek to satisfy the tangential interpolation conditions (14) and (15) are computed as

$$\begin{aligned} \text{Ran} \begin{bmatrix} V_a \\ V_b \end{bmatrix} &= \text{span}_{i=1, \dots, r} \{(\sigma_i I - A_f)^{-1} B_f b_i\}, \\ \text{Ran} \begin{bmatrix} W_a \\ W_b \end{bmatrix} &= \text{span}_{i=1, \dots, r} \{(\sigma_i I - A_g^T)^{-1} C_g^T c_i\}. \end{aligned}$$

\tilde{V} and \tilde{W} are set as $\text{Ran}(\tilde{V}) \supset \text{Ran}(V_a)$ and $\text{Ran}(\tilde{W}) \supset \text{Ran}(W_a)$, $\tilde{V} = \text{orth}(\tilde{V})$, $\tilde{W} = \text{orth}(\tilde{W})$, $\tilde{W} = \tilde{W}(\tilde{V}^T \tilde{W})^{-1}$. The algorithm is stopped when the relative change in $\tilde{\lambda}_i$ stagnates, and a ROM $\tilde{H}(s)$ is identified that tends to satisfy the interpolation conditions (14) and (15).

3. Frequency-weighted \mathcal{H}_2 -optimal MOR

In this section, it is shown that the optimality conditions (6)-(8) cannot be (inherently) satisfied exactly within the projection framework. However, the conditions $\bar{X} = 0$, $\bar{Y} = 0$, and $\bar{Z} = 0$ can be achieved with the projection approach. The conditions for exactly satisfying the optimality conditions (6)-(8) are also discussed. Further, it is shown that as r increases, the deviation in the satisfaction of the optimality conditions (6)-(8) reduces as long as $\bar{X} = 0$, $\bar{Y} = 0$, and $\bar{Z} = 0$.

3.1. Limitation of Projection Framework

Let us assume at the moment for simplicity that $D_i D_i^T$, $D_o^T D_o$, \tilde{P} , and \tilde{Q} are invertible. Then it can be noted from the optimality conditions (7) and (8) that the optimal

choices of \tilde{B} and \tilde{C} should satisfy the following

$$\begin{aligned}\tilde{B} &= -\tilde{Q}^{-1}Q_{12}^TB - \tilde{Q}^{-1}Y(D_iD_i^T)^{-1}, \\ \tilde{C} &= CP_{12}\tilde{P}^{-1} + (D_o^TD_o)^{-1}Z\tilde{P}^{-1}.\end{aligned}$$

Since \tilde{B} and \tilde{C} are computed as \tilde{W}^TB and $C\tilde{V}$, respectively, in the projection framework, the matrices \tilde{V} and \tilde{W} should be selected as $\tilde{V} = P_{12}\tilde{P}^{-1}$ and $\tilde{W} = -Q_{12}\tilde{Q}^{-1}$ (note that \tilde{P} and \tilde{Q} are symmetric). Moreover, this selection ensures that $\tilde{Y} = 0$ and $\tilde{Z} = 0$ without assuming that $D_iD_i^T$ and $D_o^TD_o$ are invertible. Since P_{12} , Q_{12} , \tilde{P} , and \tilde{Q} depend on the unknown $(\tilde{A}, \tilde{B}, \tilde{C})$, the problem is nonconvex. Nevertheless, if such a solution is found within the projection framework, $\tilde{X} = 0$ due to the oblique projection condition $\tilde{W}^T\tilde{V} = I$. The deviations in the satisfaction of optimality conditions (6)-(8) are then quantified by X , Y , and Z . If $X = 0$, $Y = 0$, and $Z = 0$, the problem can be solved within the projection framework by finding the reduction subspaces that ensure $\tilde{V} = P_{12}\tilde{P}^{-1}$, $\tilde{W} = -Q_{12}\tilde{Q}^{-1}$, and $\tilde{W}^T\tilde{V} = I$. The reduction subspaces \tilde{V} and \tilde{W} have no influence on P_{13} , P_i , Q_{14} , and Q_o . There seems no straightforward way to influence P_{23} , P_{24} , P_{34} , Q_{23} , Q_{24} , and Q_{34} using \tilde{V} and \tilde{W} so that X , Y , and Z become zeros. Further, it is shown in (Hurak et al., 2001; Sreeram, 2002; Sreeram and Sahlan, 2012) that the nonzero cross-terms P_{13} , P_{23} , Q_{14} , and Q_{24} are inherent to the frequency-weighted MOR problem, and the effect of frequency-weights vanishes when these are zeros. Therefore, at best, we can ensure $\tilde{X} = 0$, $\tilde{Y} = 0$, and $\tilde{Z} = 0$ within the projection framework.

FWITIA is not motivated by the optimality conditions (6)-(8). Instead, it follows the system theory perspective that ensuring small $\|E(s)W_i(s)\|_{\mathcal{H}_2}$ and $\|W_o(s)E(s)\|_{\mathcal{H}_2}$ generally ensures that $\|E_w(s)\|_{\mathcal{H}_2}$ is also small. Note that \mathcal{H}_2 -norm, unlike \mathcal{H}_∞ -norm, does not enjoy submultiplicative property, and hence,

$$\|E_w(s)\|_{\mathcal{H}_2} \leq \|E(s)W_i(s)\|_{\mathcal{H}_2} + \|W_o(s)E(s)\|_{\mathcal{H}_2}$$

does not hold in general. However, it can be shown that $\tilde{Y} = 0$ and $\tilde{Z} = 0$ is equivalent to ensuring that the gradients of the additive components of $\|E_w(s)\|_{\mathcal{H}_2}^2$ with respect to \tilde{B} and \tilde{C} , respectively, become zero. This is established in Proposition 3.1.

Proposition 3.1. *Let us split $\|E_w(s)\|_{\mathcal{H}_2}^2$ into its additive components as $\|E_w(s)\|_{\mathcal{H}_2}^2 = \mathcal{J}_1 + \mathcal{J}_2 = \mathcal{J}_3 + \mathcal{J}_4$ where*

$$\begin{aligned}\mathcal{J}_1 &= \text{tr}(D_oCPC^TD_o^T + D_o\tilde{C}\tilde{P}\tilde{C}^TD_o^T - 2D_oCP_{12}\tilde{C}^TD_o^T), \\ \mathcal{J}_2 &= \text{tr}(C_oP_oC_o^T + 2D_oCP_{14}C_o^T - 2D_o\tilde{C}P_{24}C_o^T), \\ \mathcal{J}_3 &= \text{tr}(D_i^TB^TQB D_i + D_i^T\tilde{B}^T\tilde{Q}\tilde{B}D_i + 2D_i^TB^TQ_{12}\tilde{B}D_i), \\ \mathcal{J}_4 &= \text{tr}(B_i^TQ_iB_i + 2D_i^TB^TQ_{13}B_i + D_i^T\tilde{B}^TQ_{23}B_i).\end{aligned}$$

Then $\frac{\partial}{\partial \tilde{C}}\mathcal{J}_1 = 0$ and $\frac{\partial}{\partial \tilde{B}}\mathcal{J}_3 = 0$ when $\tilde{Z} = 0$ and $\tilde{Y} = 0$, respectively.

Proof. Let us denote the first-order derivative of \mathcal{J}_3 with respect to \tilde{B} as $\Delta_{\mathcal{J}_3}^{\tilde{B}}$ and

the differential of \tilde{B} as $\Delta_{\tilde{B}}$. Then

$$\begin{aligned}\Delta_{\tilde{J}_3}^{\tilde{B}} &= \text{tr}(2D_i^T \Delta_{\tilde{B}}^T \tilde{Q} \tilde{B} D_i + 2D_i^T B^T Q_{12} \Delta_{\tilde{B}} D_i) \\ &= \text{tr}\left((2D_i D_i^T \tilde{B} \tilde{Q} + 2D_i D_i^T B^T Q_{12}) \Delta_{\tilde{B}}\right).\end{aligned}$$

Since $\Delta_{\tilde{J}_3}^{\tilde{B}} = \text{tr}\left(\left(\frac{\partial}{\partial \tilde{B}} \mathcal{J}_3\right)^T \Delta_{\tilde{B}}\right)$, $\frac{\partial}{\partial \tilde{B}} \mathcal{J}_3 = 2\bar{Y} D_i D_i^T$. Thus when $\bar{Y} = 0$, $\frac{\partial}{\partial \tilde{B}} \mathcal{J}_3 = 0$.

Now, let us denote the first-order derivative of \mathcal{J}_1 with respect to \tilde{C} as $\Delta_{\tilde{J}_1}^{\tilde{C}}$ and the differential of \tilde{C} as $\Delta_{\tilde{C}}$. Then

$$\begin{aligned}\Delta_{\tilde{J}_1}^{\tilde{C}} &= \text{tr}(2D_o \Delta_{\tilde{C}} \tilde{P} \tilde{C}^T D_o^T - 2D_o C P_{12} \Delta_{\tilde{C}}^T D_o^T) \\ &= \text{tr}\left((2\tilde{P} \tilde{C}^T D_o^T D_o - 2P_{12}^T C^T D_o^T D_o) \Delta_{\tilde{C}}\right).\end{aligned}$$

Since $\Delta_{\tilde{J}_1}^{\tilde{C}} = \text{tr}\left(\left(\frac{\partial}{\partial \tilde{C}} \mathcal{J}_1\right)^T \Delta_{\tilde{C}}\right)$, $\frac{\partial}{\partial \tilde{C}} \mathcal{J}_1 = 2D_o^T D_o \bar{Z}$. Thus when $\bar{Z} = 0$, $\frac{\partial}{\partial \tilde{C}} \mathcal{J}_1 = 0$. This completes the proof. \square

Although this was not recognized in (Zulfikar et al., 2019), it is evident now that FWITIA is not completely heuristic in terms of seeking to ensure that $\|E_w(s)\|_{\mathcal{H}_2}^2$ is small. Note that FWITIA seeks to ensure that $\bar{Y} = 0$ and $\bar{Z} = 0$ by satisfying the tangential interpolation conditions (14) and (15). However, (14) and (15) require $F[\tilde{H}(s)]$ and $G[\tilde{H}(s)]$ to maintain the structure of $F[H(s)]$ and $G[H(s)]$ given in (11)-(13), which is not possible in general. Therefore, FWITIA may not satisfy the interpolation conditions (14) and (15) exactly, and thus $\bar{Y} \approx 0$ and $\bar{Z} \approx 0$ upon convergence.

An interesting parallel should be noted that the nonzero cross-terms P_{13} , P_{23} , Q_{14} , and Q_{24} inhibit FWBT to inherit the stability preservation and Hankel singular values retention properties of BT (Ghafoor et al., 2007; Sreeram and Sahlan, 2012). Here also, the nonzero cross-terms inhibit the projection framework to satisfy the first-order optimality conditions exactly, which is possible in case of the standard \mathcal{H}_2 -optimal MOR problem.

3.2. Conditions for Exact Satisfaction of the Optimality Conditions

As seen already that to ensure $\bar{X} = 0$, $\bar{Y} = 0$, and $\bar{Z} = 0$, we need to find the reduction subspaces $\tilde{V} = P_{12} \tilde{P}^{-1}$ and $\tilde{W} = -Q_{12} \tilde{Q}^{-1}$ that ensures the oblique projection condition $\tilde{W}^T \tilde{V} = I$. By expanding the Lyapunov equations (4) and (5) according to the structure of (A_w, B_w, C_w) in (3), it can be noted that P_{23} , \tilde{P} , P_{12} , Q_{24} , \tilde{Q} , and Q_{12} solve the following Sylvester equations

$$\tilde{A} P_{23} + P_{23} A_i^T + \tilde{B} (C_i P_i + D_i B_i^T) = 0, \quad (16)$$

$$\tilde{A} \tilde{P} + \tilde{P} \tilde{A}^T + \tilde{B} C_i P_{23}^T + P_{23} C_i^T \tilde{B}^T + \tilde{B} D_i D_i^T \tilde{B}^T = 0, \quad (17)$$

$$A P_{12} + P_{12} \tilde{A}^T + B C_i P_{23}^T + P_{13} C_i^T \tilde{B}^T + B D_i D_i^T \tilde{B}^T = 0, \quad (18)$$

$$\tilde{A}^T Q_{24} + Q_{24} A_o - \tilde{C}^T (B_o^T Q_o + D_o^T C_o) = 0, \quad (19)$$

$$\tilde{A}^T \tilde{Q} + \tilde{Q} \tilde{A} - \tilde{C}^T B_o^T Q_{24}^T - Q_{24} B_o \tilde{C} + \tilde{C}^T D_o^T D_o \tilde{C} = 0, \quad (20)$$

$$A^T Q_{12} + Q_{12} \tilde{A} + C^T B_o^T Q_{24}^T - Q_{14} B_o \tilde{C} - C^T D_o^T D_o \tilde{C} = 0. \quad (21)$$

If the ROM is obtained using the oblique projection $\Pi = -P_{12}\tilde{P}^{-1}\tilde{Q}^{-1}Q_{12}^T$ with $\tilde{V} = P_{12}\tilde{P}^{-1}$ and $\tilde{W} = -Q_{12}\tilde{Q}^{-1}$, (2) and the equations (16)-(21) can be viewed as two coupled system of equations, i.e.,

$$\begin{aligned}(\tilde{A}, \tilde{B}, \tilde{C}) &= f(P_{12}, Q_{12}, \tilde{P}, \tilde{Q}), \\(P_{12}, Q_{12}, \tilde{P}, \tilde{Q}) &= g(\tilde{A}, \tilde{B}, \tilde{C}).\end{aligned}$$

Clearly, the fixed points of $(\tilde{A}, \tilde{B}, \tilde{C}) = f(g(\tilde{A}, \tilde{B}, \tilde{C}))$ ensure that $\bar{X} = 0$, $\bar{Y} = 0$, and $\bar{Z} = 0$ if the condition for oblique projection $\tilde{W}^T\tilde{V} = I$ is satisfied. We now show in the next theorem that these fix points satisfy the optimality conditions (6)-(8) if $CP_{13} - \tilde{C}P_{23} = 0$ and $B^TQ_{14} + \tilde{B}^TQ_{24} = 0$.

Theorem 3.2. *Let \tilde{A} be Hurwitz and $(\tilde{A}, \tilde{B}, \tilde{C})$ be a fixed point of $(\tilde{A}, \tilde{B}, \tilde{C}) = f(g(\tilde{A}, \tilde{B}, \tilde{C}))$. Also, let that \tilde{P} and \tilde{Q} are invertible at the fixed point, and the fixed point is obtained by using the oblique projection $\Pi = -P_{12}\tilde{P}^{-1}\tilde{Q}^{-1}Q_{12}^T$ with $\tilde{V} = P_{12}\tilde{P}^{-1}$ and $\tilde{W} = -Q_{12}\tilde{Q}^{-1}$. Then $(\tilde{A}, \tilde{B}, \tilde{C})$ satisfies the first-order optimality conditions (6)-(8) provided $CP_{13} - \tilde{C}P_{23} = 0$ and $B^TQ_{14} + \tilde{B}^TQ_{24} = 0$.*

Proof. We need to show that when $CP_{13} - \tilde{C}P_{23} = 0$ and $B^TQ_{14} + \tilde{B}^TQ_{24} = 0$, $X = 0$, $Y = 0$, and $Z = 0$ at the fixed points of $(\tilde{A}, \tilde{B}, \tilde{C}) = f(g(\tilde{A}, \tilde{B}, \tilde{C}))$. By expanding the Lyapunov equation (4), one can note that P_{34} and P_{24} satisfy the following Sylvester equations

$$\begin{aligned}A_iP_{34} + P_{34}A_o^T + (P_{13}^TC^T - P_{23}^T\tilde{C}^T)B_o^T &= 0, \\ \tilde{A}P_{24} + P_{24}A_o^T + \tilde{B}C_iP_{34} + (P_{12}^TC^T - \tilde{P}\tilde{C}^T)B_o^T &= 0.\end{aligned}$$

Since $\bar{Z} = 0$ and $CP_{13} - \tilde{C}P_{23} = 0$, we get

$$A_iP_{34} + P_{34}A_o^T = 0 \text{ and } \tilde{A}P_{24} + P_{24}A_o^T + \tilde{B}C_iP_{34} = 0.$$

Thus $P_{34} = 0$ and $P_{24} = 0$.

It can be noted by expanding the Lyapunov equation (5) that Q_{34} and Q_{23} solve the following Sylvester equations

$$\begin{aligned}A_i^TQ_{34} + Q_{34}A_o + C_i^T(B^TQ_{14} + \tilde{B}^TQ_{24}) &= 0, \\ \tilde{A}^TQ_{23} + Q_{23}A_i - \tilde{C}^TB_o^TQ_{34}^T + (\tilde{Q}\tilde{B} + Q_{12}^TB)C_i &= 0.\end{aligned}$$

Now, since $\bar{Y} = 0$ and $B^TQ_{14} + \tilde{B}^TQ_{24} = 0$, we get

$$A_i^TQ_{34} + Q_{34}A_o = 0 \text{ and } \tilde{A}^TQ_{23} + Q_{23}A_i - \tilde{C}^TB_o^TQ_{34}^T = 0.$$

Thus $Q_{34} = 0$, $Q_{23} = 0$, and therefore, $X = 0$.

Further, since $\tilde{W}^T\tilde{V} = I$, $\tilde{Q} = -Q_{12}^T\tilde{V}$ and $\tilde{P} = \tilde{W}^TP_{12}$, the matrices Y and Z become

$$\begin{aligned}Y &= Q_{12}^T(P_{13} - \tilde{V}P_{23})C_i^T = 0 \\ Z &= -B_o^T(Q_{14}^T + Q_{24}^T\tilde{W}^T)P_{12} = 0.\end{aligned}$$

Since $CP_{13} - \tilde{C}P_{23} = 0$ and $B^TQ_{14} + \tilde{B}^TQ_{24} = 0$, we can write $P_{13} - \tilde{V}P_{23} = 0$ and $Q_{14}^T + Q_{24}^T\tilde{W}^T = 0$. Thus $Y = 0$ and $Z = 0$. This completes the proof. \square

Remark 1. When $W_i(s) = I$, $Y = 0$, and the fixed point of $(\tilde{A}, \tilde{B}, \tilde{C}) = f(g(\tilde{A}, \tilde{B}, \tilde{C}))$ satisfies the optimality condition (7) exactly if \tilde{Q} is invertible at the fixed point. Similarly, when $W_o(s) = I$, $Z = 0$, and the fixed point of $(\tilde{A}, \tilde{B}, \tilde{C}) = f(g(\tilde{A}, \tilde{B}, \tilde{C}))$ satisfies the optimality condition (8) exactly if \tilde{P} is invertible at the fixed point.

Note that \tilde{P} and \tilde{Q} do not change the subspaces $\tilde{V} = P_{12}\tilde{P}^{-1}$ and $\tilde{W} = -Q_{12}\tilde{Q}^{-1}$ but only transform the basis of the subspaces P_{12} and $-Q_{12}$. Thus we can construct \tilde{V} and \tilde{W} as $\tilde{V} = P_{12}$ and $\tilde{W} = -Q_{12}$. By doing so, the invertibility of \tilde{P} and \tilde{Q} is no more required, which otherwise makes the problem quite restrictive. If the ROM is obtained by using the oblique projection $\Pi = -P_{12}Q_{12}^T$ with $\tilde{V} = P_{12}$ and $\tilde{W} = -Q_{12}$, (2) and the equations (16)-(21) can be viewed as two coupled system of equations, i.e.,

$$(\tilde{A}, \tilde{B}, \tilde{C}) = f_1(P_{12}, Q_{12}) \text{ and } (P_{12}, Q_{12}) = g_1(\tilde{A}, \tilde{B}, \tilde{C}).$$

In the next theorem, we show that the fixed points of $(\tilde{A}, \tilde{B}, \tilde{C}) = f_1(g_1(\tilde{A}, \tilde{B}, \tilde{C}))$ satisfy the optimality conditions (6)-(8) if $CP_{13} - \tilde{C}P_{23} = 0$ and $B^TQ_{14} + \tilde{B}^TQ_{24} = 0$.

Theorem 3.3. *Let \tilde{A} be Hurwitz and $(\tilde{A}, \tilde{B}, \tilde{C})$ be a fixed point of $(\tilde{A}, \tilde{B}, \tilde{C}) = f_1(g_1(\tilde{A}, \tilde{B}, \tilde{C}))$ obtained by using the oblique projection $\Pi = -P_{12}Q_{12}^T$ with $\tilde{V} = P_{12}$ and $\tilde{W} = -Q_{12}$. Then $(\tilde{A}, \tilde{B}, \tilde{C})$ satisfies the first-order optimality conditions (6)-(8) provided $CP_{13} - \tilde{C}P_{23} = 0$ and $B^TQ_{14} + \tilde{B}^TQ_{24} = 0$.*

Proof. Since the fixed points of $(\tilde{A}, \tilde{B}, \tilde{C}) = f_1(g_1(\tilde{A}, \tilde{B}, \tilde{C}))$ are obtained by using the oblique projection $\Pi = -P_{12}Q_{12}^T$, the following holds $CP_{12} - \tilde{C} = 0$, $Q_{12}^TB + \tilde{B} = 0$, and $Q_{12}^TP_{12} + I = 0$ at the fixed points. We first show that $\bar{X} = 0$, $\bar{Y} = 0$, and $\bar{Z} = 0$ at the fixed points of $(\tilde{A}, \tilde{B}, \tilde{C}) = f_1(g_1(\tilde{A}, \tilde{B}, \tilde{C}))$ if $CP_{13} - \tilde{C}P_{23} = 0$ and $B^TQ_{14} + \tilde{B}^TQ_{24} = 0$. By multiplying (18) with \tilde{W}^T from the left, we get

$$\tilde{W}^TAP_{12} + \tilde{W}^TP_{12}\tilde{A}^T + \tilde{W}^TBC_iP_{23}^T + \tilde{W}^TP_{13}C_i^T\tilde{B}^T + \tilde{W}^TBD_iD_i^T\tilde{B}^T = 0.$$

Note that $\tilde{W}^TP_{12} = \tilde{W}^T\tilde{V} = I$. Also, note that $\tilde{W}^TP_{13} = P_{23}$, since $CP_{13} - \tilde{C}P_{23} = C(P_{13} - \tilde{V}P_{23}) = 0$. Thus

$$\tilde{A} + \tilde{A}^T + \tilde{B}C_iP_{23}^T + P_{23}C_i^T\tilde{B}^T + \tilde{B}D_iD_i^T\tilde{B}^T = 0.$$

Due to uniqueness, $\tilde{P} = I$, and thus $\bar{Z} = 0$.

By multiplying (21) with \tilde{V}^T from the left, we get

$$\tilde{V}^TA^TQ_{12} + \tilde{V}^TQ_{12}\tilde{A} + \tilde{V}^TC^TB_o^TQ_{24}^T - \tilde{V}^TQ_{14}B_o\tilde{C} - \tilde{V}^TC^TD_o^TD_o\tilde{C} = 0.$$

Note that $Q_{14} = -\tilde{W}Q_{24}$ and $\tilde{V}^TQ_{14} = -Q_{24}$ since $B^T(Q_{14} + \tilde{W}Q_{24}) = 0$. Also, note that $\tilde{V}^T\tilde{W} = -\tilde{V}^TQ_{12} = I$. Thus

$$-\tilde{A}^T - \tilde{A} + \tilde{C}^TB_o^TQ_{24}^T + Q_{24}B_o\tilde{C} - \tilde{C}^TD_o^TD_o\tilde{C} = 0.$$

Due to uniqueness, $\tilde{Q} = I$, and thus $\bar{Y} = 0$ and $\bar{X} = 0$.

It is now left to show that $X = 0$, $Y = 0$, and $Z = 0$. From Theorem 3.2, we know that when $\tilde{Y} = 0$, $\tilde{Z} = 0$, $P_{13} = \tilde{V}P_{23}$, and $Q_{14} = -\tilde{W}Q_{24}$, the matrices $P_{34} = 0$, $Q_{23} = 0$ and $X = 0$. Further, since $\tilde{P} = I$, and $\tilde{Q} = I$, Y and Z become

$$Y = (Q_{12}^T P_{13} + P_{23})C_i^T \text{ and } Z = B_o^T(Q_{14}^T P_{12} + Q_{24}^T).$$

Since $P_{13} - \tilde{V}P_{23} = 0$ and $Q_{14} + \tilde{W}Q_{24} = 0$, the matrices $Y = 0$ and $Z = 0$. This completes the proof. \square

Remark 2. For the oblique projection $\Pi = -P_{12}\tilde{P}^{-1}\tilde{Q}^{-1}Q_{12}^T$, the fixed points of $(\tilde{A}, \tilde{B}, \tilde{C}) = f(g(\tilde{A}, \tilde{B}, \tilde{C}))$ ensures $\tilde{X} = 0$, $\tilde{Y} = 0$, and $\tilde{Z} = 0$ regardless of whether the conditions $P_{13} = \tilde{V}P_{23}$ and $Q_{14} = -\tilde{W}Q_{24}$ hold or not. However, for the oblique projection $\Pi = -P_{12}Q_{12}^T$, the fixed points of $(\tilde{A}, \tilde{B}, \tilde{C}) = f_1(g_1(\tilde{A}, \tilde{B}, \tilde{C}))$ ensures $\tilde{X} = 0$, $\tilde{Y} = 0$, and $\tilde{Z} = 0$ only if $P_{13} = \tilde{V}P_{23}$ and $Q_{14} = -\tilde{W}Q_{24}$ also hold. Therefore, although the reduction subspaces \tilde{V} and \tilde{W} span the same subspace in both cases, the change of basis in the latter case incurs deviations in $\tilde{X} = 0$, $\tilde{Y} = 0$, and $\tilde{Z} = 0$ if the conditions $P_{13} = \tilde{V}P_{23}$ and $Q_{14} = -\tilde{W}Q_{24}$ are violated.

By expanding the Lyapunov equations (4) and (5), one can note that P_{13} and Q_{14} solve the following Sylvester equations

$$AP_{13} + P_{13}A_i^T + B(C_iP_i + D_iB_i^T) = 0, \quad (22)$$

$$A^TQ_{14} + Q_{14}A_o + C^T(B_o^TQ_o + D_o^TC_o) = 0. \quad (23)$$

Thus $\tilde{V}P_{23}$ and $-\tilde{W}Q_{24}$ can be seen as Petrov-Galerkin approximations of P_{13} and Q_{14} in the following sense

$$\begin{aligned} & \text{Ran}(\tilde{A}\tilde{V}P_{23} + \tilde{V}P_{23}A_i^T + B(C_iP_i + D_iB_i^T)) \perp \text{Ran}(\tilde{W}), \\ & \text{Ran}(A^T\tilde{W}Q_{24} + \tilde{W}Q_{24}A_o - C^T(B_o^TQ_o + D_o^TC_o)) \perp \text{Ran}(\tilde{V}). \end{aligned}$$

In general, $P_{13} \neq \tilde{V}P_{23}$ and $Q_{14} \neq -\tilde{W}Q_{24}$, and therefore, $CP_{13} - \tilde{C}P_{23} \neq 0$ and $B^TQ_{14} + \tilde{B}^TQ_{24} \neq 0$. To achieve a nearly optimum ROM, we need to find fixed points of $(\tilde{A}, \tilde{B}, \tilde{C}) = f_1(g_1(\tilde{A}, \tilde{B}, \tilde{C}))$ by using the oblique projection $\Pi = \tilde{V}\tilde{W}^T$, which also provides good Petrov-Galerkin approximations of P_{13} and Q_{14} as $\tilde{V}P_{23} \approx P_{13}$ and $-\tilde{W}Q_{24} \approx Q_{14}$.

Remark 3. When $W_i(s)$ and $W_o(s)$ are co-inner and inner functions, respectively, the matrices $P_{13} = 0$, $P_{23} = 0$, $Q_{14} = 0$, and $Q_{24} = 0$ (Sahlan et al., 2007; Sreeram, 2002; Sreeram and Sahlan, 2012). Thus $CP_{13} - \tilde{C}P_{23} = 0$ and $B^TQ_{14} + \tilde{B}^TQ_{24} = 0$, and the fixed points of $(\tilde{A}, \tilde{B}, \tilde{C}) = f_1(g_1(\tilde{A}, \tilde{B}, \tilde{C}))$ satisfy the optimality conditions (6)-(8) exactly.

3.3. Deviation in the Optimality Conditions

We now show that as the order of the ROM increases, the fixed points of $(\tilde{A}, \tilde{B}, \tilde{C}) = f_1(g_1(\tilde{A}, \tilde{B}, \tilde{C}))$ implicitly ensures that $P_{13} \approx \tilde{V}P_{23}$ and $Q_{14} \approx -\tilde{W}Q_{24}$. Thus the deviation in the satisfaction of the optimality conditions (6)-(8) decays as the order of ROM increases.

To observe this, note that

$$\|E(s)W_i(s)\|_{\mathcal{H}_2}^2 = \text{trace}(CPC^T - 2CP_{12}\tilde{C}^T + \tilde{C}\tilde{P}\tilde{C}^T).$$

When $\bar{Z} = 0$, $\|E(s)W_i(s)\|_{\mathcal{H}_2}^2$ becomes

$$\|E(s)W_i(s)\|_{\mathcal{H}_2}^2 = \text{trace}(CPC^T - \tilde{C}\tilde{P}\tilde{C}^T) = \text{trace}(C(P - \tilde{V}\tilde{P}\tilde{V})C^T).$$

Thus as the order of ROM increases and $\|E(s)W_i(s)\|_{\mathcal{H}_2}^2$ decreases, $\hat{P} = \tilde{V}\tilde{P}\tilde{V}$ approaches P . Also, since

$$\|W(s)E(s)\|_{\mathcal{H}_2}^2 = \text{trace}(B^TQB + 2B^TQ_{12}\tilde{B} + \tilde{B}^T\tilde{Q}\tilde{B}),$$

$\bar{Y} = 0$, $\|W_o(s)E(s)\|_{\mathcal{H}_2}^2$ becomes

$$\|W_o(s)E(s)\|_{\mathcal{H}_2}^2 = \text{trace}(B^TQB - \tilde{B}^T\tilde{Q}\tilde{B}) = \text{trace}(B^T(Q - \tilde{W}\tilde{Q}\tilde{W}^T)B).$$

As the order of ROM increases and $\|W_o(s)E(s)\|_{\mathcal{H}_2}^2$ decreases, $\hat{Q} = \tilde{W}\tilde{Q}\tilde{W}^T$ approaches Q .

P and Q solve the following Lyapunov equations

$$AP + PA^T + BC_iP_{13}^T + P_{13}C_i^TB^T + BD_iD_i^TB^T = 0, \quad (24)$$

$$A^TQ + QA + C^TB_o^TQ_{14}^T + Q_{14}B_oC + C^TD_o^TD_oC = 0. \quad (25)$$

Let the residuals R_1 and R_2 be defined as

$$\begin{aligned} R_1 &= A\hat{P} + \hat{P}A^T + BC_iP_{13}^T + P_{13}C_i^TB^T + BD_iD_i^TB^T, \\ R_2 &= A^T\hat{Q} + \hat{Q}A + C^TB_o^TQ_{14}^T + Q_{14}B_oC + C^TD_o^TD_oC. \end{aligned}$$

As \hat{P} and \hat{Q} approach P and Q , respectively, R_1 and R_2 approach zero. Further, when $R_1 \approx 0$ and $R_2 \approx 0$, the Petrov-Galerkin conditions $\tilde{W}^TR_1\tilde{W} \approx 0$ and $\tilde{V}^TR_2\tilde{V} \approx 0$ also hold approximately, which imply that $\tilde{W}^TP_{13} \approx P_{23}$ and $\tilde{V}^TQ_{14} \approx -Q_{24}$. The singular values of P and Q decay rapidly in the weighted case (Benner et al., 2016; Kürschner, 2018). Thus $\|R_1\|$ and $\|R_2\|$ are expected to decay quickly for a relatively smaller value of r due to low numerical rank of P and Q . Therefore, the conditions $\tilde{V}P_{23} \approx P_{13}$ and $-\tilde{W}Q_{24} \approx Q_{14}$ are expected to be met without having to increase the value of r too much. In short, a compact ROM that nearly satisfies the optimality conditions (6)-(8) can be obtained with the oblique projection $\Pi = -P_{12}Q_{12}^T$.

4. Frequency-weighted \mathcal{H}_2 -suboptimal MOR

In this section, a fixed point iteration algorithm is proposed, which on convergence tends to satisfy $\bar{X} = 0$, $\bar{Y} = 0$, and $\bar{Z} = 0$, and therefore the resulting ROM tends to satisfy the optimality conditions (6)-(8).

4.1. Fixed-point Iteration Algorithm

The fixed points of $(\tilde{A}, \tilde{B}, \tilde{C}) = f_1(g_1(\tilde{A}, \tilde{B}, \tilde{C}))$ can be found by using the fixed point iteration algorithm with an additional constraint that P_{12} and $-Q_{12}$ satisfy the oblique projection condition $-Q_{12}^T P_{12} = I$. To ensure that $\tilde{W}^T \tilde{V} = I$, most of the \mathcal{H}_2 -optimal MOR algorithms use the correction equation $\tilde{W} = \tilde{W}(\tilde{V}^T \tilde{W})^{-1}$. Theoretically, it does ensure that $\tilde{W}^T \tilde{V} = I$, however, it becomes numerically unstable even for small systems (Benner et al., 2011). A more robust approach is to take the geometric interpretation of $\tilde{W}^T \tilde{V} = I$, i.e., the columns of \tilde{W} and \tilde{V} form biorthogonal basis of a subspace in \mathbb{R}^n (Benner et al., 2011). Therefore, we use biorthogonal Gram-Schmidt method (steps 6-11 of Algorithm 1) to ensure that $\tilde{W}^T \tilde{V} = I$ for better numerical properties. The pseudo code of our approach is given in Algorithm 1, which is referred to as the frequency-weighted \mathcal{H}_2 -suboptimal MOR algorithm (FWHMOR).

Algorithm 1 FWHMOR

Input: Original system: (A, B, C) ; Input weight: (A_i, B_i, C_i, D_i) ; Output weight: (A_o, B_o, C_o, D_o) , Initial guess: $(\tilde{A}, \tilde{B}, \tilde{C})$.

Output: ROM $(\tilde{A}, \tilde{B}, \tilde{C})$.

1: Compute P_i and Q_o by solving

$$\begin{aligned} A_i P_i + P_i A_i^T + B_i B_i^T &= 0, \\ A_o^T Q_o + Q_o A_o + C_o^T C_o &= 0. \end{aligned}$$

2: Compute P_{13} and Q_{14} from the equations (22) and (23), respectively.

3: **while** (not converged) **do**

4: Compute P_{23} and Q_{24} from the equations (16) and (19), respectively.

5: Compute P_{12} and Q_{12} from the equations (18) and (21), respectively.

6: **for** $i = 1, \dots, r$ **do**

7: $v = P_{12}(:, i)$, $v = \prod_{k=1}^i (I + P_{12}(:, k) Q_{12}(:, k)^T) v$.

8: $w = -Q_{12}(:, i)$, $w = \prod_{k=1}^i (I + Q_{12}(:, k) P_{12}(:, k)^T) w$.

9: $v = \frac{v}{\|v\|_2}$, $w = \frac{w}{\|w\|_2}$, $v = \frac{v}{w^T v}$.

10: $\tilde{V}(:, i) = v$, $\tilde{W}(:, i) = w$.

11: **end for**

12: $\tilde{A} = \tilde{W}^T A \tilde{V}$, $\tilde{B} = \tilde{W}^T B$, $\tilde{C} = C \tilde{V}$.

13: **end while**

Remark 4. FWHMOR provides approximations of P and Q as \hat{P} and \hat{Q} , respectively, which can be used in FWBT to save some computational cost by avoiding the computation of large-scale Lyapunov equations (24) and (25).

4.2. Connection with FWITIA

Let us assume that FWITIA and FWHMOR have converged, and (V_a, W_a) and (\tilde{V}, \tilde{W}) are the respective reduction subspaces of the last iteration. Also, suppose $\tilde{H}(s)$ has simple poles. Let us denote the spectral factorization of \tilde{A} as $\tilde{A} = R S R^{-1}$ where $S = \text{diag}(\tilde{\lambda}_1, \dots, \tilde{\lambda}_r)$. Now define L_i and L_o as $L_i = \tilde{B}^T R^{-*} = [\tilde{r}_1 \ \dots \ \tilde{r}_r]$ and $L_o = \tilde{C} R = [\tilde{l}_1 \ \dots \ \tilde{l}_r]$, respectively. Owing to the connection of Sylvester equations

and rational Krylov subspaces (Panzer, 2014; Wolf, 2014), it is shown in (Zulfiqar et al., 2019) that V_a and W_a in FWITIA satisfy the following Sylvester equations

$$\begin{aligned} AV_a + V_a S^* + BC_i V_b^T + P_{13} C_i^T L_i + BD_i D_i^T L_i &= 0, \\ A^T W_a + W_a S + C^T B_i^T W_b^T + Q_{14} B_i L_o + C^T D_o^T D_o L_o &= 0 \end{aligned}$$

where

$$\begin{aligned} SV_b + V_b A_i^T + L_i^* (C_i P_i + D_i B_i^T) &= 0, \\ S^* W_b + W_b A_o + L_o^T (B_o^T Q_o + D_o^T C_o) &= 0. \end{aligned}$$

By putting $\tilde{A} = RSR^{-1}$ in (16) and (18), pre-multiplying (16) with R^{-1} , and post-multiplying (18) with R^{-*} , one can note that the following Sylvester equations hold

$$\begin{aligned} SR^{-1} P_{23} + R^{-1} P_{23} A_i^T + L_i^* (C_i P_i + D_i B_i^T) &= 0, \\ AP_{12} R^{-*} + P_{12} R^{-*} S^* + BC_i P_{23}^T R^{-*} + P_{13} C_i^T L_i + BD_i D_i^T L_i &= 0. \end{aligned}$$

Due to uniqueness, $V_a = P_{12} R^{-*}$ and $V_b = R^{-1} P_{23}$. Similarly, by putting $\tilde{A} = RSR^{-1}$ (19) and (21), pre-multiplying (19) with R^* , and post-multiplying (21) with R^{-*} , one can note that the following Sylvester equations hold

$$\begin{aligned} S^* R^* Q_{24} + R^* Q_{24} A_o - L_o^T (B_o^T Q_o + D_o^T C_o) &= 0, \\ A^T Q_{12} R + Q_{12} RS - C^T B_i^T Q_{24}^T R - Q_{14} B_i L_o - C^T D_o^T D_o L_o &= 0. \end{aligned}$$

Due to uniqueness, $W_a = -Q_{12} R$ and $W_b = -R^* Q_{24}$. Since R only changes the basis of V_a and W_a , the columns of \tilde{V} and \tilde{W} in FWHMOR span the same subspaces as spanned by V_a and W_a , respectively, in FWITIA. Therefore, the ROM constructed by FWHMOR satisfies the tangential interpolation conditions (14) and (15) upon convergence like FWITIA, provided $P_{13} = \tilde{V} P_{23}$ and $Q_{14} = -\tilde{W} Q_{24}$. However, there are some notable numerical differences between FWHMOR and FWITIA. FWHMOR does not require $H(s)$ and $\tilde{H}(s)$ to have simple poles, unlike FWITIA. Thus \tilde{A} does not need to be diagonalizable in FWHMOR. Therefore, FWITIA can be considered equivalent to FWHMOR if $H(s)$ and $\tilde{H}(s)$ have simple poles. The spectral factorization of \tilde{A} in every iteration of FWITIA may cause numerical ill-conditioning (Benner et al., 2011). Moreover, FWITIA uses the correction equation $\tilde{W} = \tilde{W}(\tilde{V}^T \tilde{W})^{-1}$ to ensure the oblique projection condition $\tilde{W}^T \tilde{V} = I$, whereas FWHMOR uses numerically more stable biorthogonal Gram-Schmidt (Benner et al., 2011) to achieve that. In short, FWHMOR is numerically more general and stable algorithm than FWITIA, though both span the same subspaces. Moreover, the results of Section 3 provide the theoretical foundation for FWITIA in terms of seeking to satisfy the optimality conditions (6)-(8). Hence, FWITIA is no more a heuristic generalization of (Van Dooren et al., 2008) but an interpolation framework for the frequency-weighted \mathcal{H}_2 -optimal MOR problem.

4.3. Computational Aspects

We now discuss some computational aspects of FWHMOR to be considered for its efficient numerical implementation.

4.3.1. Initial Guess

The initial guess of the ROM can be made arbitrarily, for instance, by direct truncation of the original state-space realization. However, a good choice of the initial ROM generally has a positive impact on the performance of the fixed point iteration methods. Therefore, it is recommended to generate the initial guess by using the eigensolver proposed in (Rommes and Martins, 2006). Since the mirror images of the poles with large residues have a big contribution to the \mathcal{H}_2 -norm, the initial guess can be generated with the eigensolver proposed in (Rommes and Martins, 2006) by projecting $H(s)$ onto the dominant eigenspace of A . Another option is to compute the initial ROM by using the low-rank approximation methods in (Ahmad et al., 2010; Benner and Kürschner, 2014) such that it provides good Petrov-Galerkin approximations of P_{13} and Q_{14} as $\tilde{V}P_{23}$ and $-\tilde{W}Q_{24}$. This ensures that $\|P_{13} - \tilde{V}P_{23}\|$ and $\|Q_{14} + \tilde{W}Q_{24}\|$ are small to begin with.

4.3.2. Convergence and Stopping Criteria

Like in most of the \mathcal{H}_2 -optimal MOR algorithms, the convergence is not guaranteed in FWHMOR. Therefore, a good stopping criterion is required to stop the algorithm in case it does not converge within admissible time. The stopping criterion should have two main properties: (i) It should be easily computable (ii) It should quickly indicate that the error has dropped appreciably. These two properties make sure that the computation of stopping criteria is not a computational burden in itself, and it can save computational effort by indicating that the algorithm is not improving the accuracy of ROM any further. Owing to connection between FWITIA and FWHMOR, the relative change in eigenvalues of \tilde{A} can be used as the stopping criterion. Due to the small size of \tilde{A} , this can be achieved accurately and cheaply using QZ -method. $\|\tilde{X}\|_2$ can also be used as a stopping criterion. The computation of \tilde{P} and \tilde{Q} in $\|\tilde{X}\|_2$ requires solutions of two small-scale Lyapunov equations, i.e., (17) and (20), which can be done cheaply. Also, note that from a pragmatic perspective, achieving less $\|E_w(s)\|_{\mathcal{H}_2}^2$ is the main objective and not the local optimum in itself. Thus the stopping criterion can be based directly on the error itself. However, the computation of $\|E_w(s)\|_{\mathcal{H}_2}^2$ in each iteration is an expensive operation in a large-scale setting. We have discussed in Section 3 that $\tilde{Y} = 0$ and $\tilde{Z} = 0$ essentially minimize $\|W(s)E(s)\|_{\mathcal{H}_2}^2$ and $\|E(s)V(s)\|_{\mathcal{H}_2}^2$, respectively. Therefore, one can use the relative changes in $e_1 = \text{tr}(2CP_{12}\tilde{C}^T - \tilde{C}\tilde{P}\tilde{C}^T)$ and $e_2 = \text{tr}(-2B^TQ_{12}\tilde{B} - \tilde{B}^T\tilde{Q}\tilde{B})$ as the stopping criteria. The algorithm can be stopped when relative changes in e_1 and e_2 stagnate because this indicates that $\|E(s)V(s)\|_{\mathcal{H}_2}^2$ and $\|W(s)E(s)\|_{\mathcal{H}_2}^2$ are not changing. Another criterion for stopping the algorithm can be the number of iterations or computational time. If the other stopping criteria are not achieved within the maximum allowable number of iterations or admissible time, the algorithm can be stopped prematurely.

4.3.3. Computational Cost

The computational cost of FWHMOR depends on several factors. In step 1, P_i and Q_o can be computed cheaply if n_i and n_o are small. However, if the weights $W_i(s)$ and $W_o(s)$ are large-scale transfer functions, P_i and Q_o should be replaced with their low-rank approximations, for instance, by using the toolboxes (Penzl, 1999b; Saak et al., 2010). In step 2, P_{13} and Q_{14} can be computed within admissible time if n_i and n_o are small due to the *sparse-dense* structure of the Sylvester equations (22) and (23) (Panzer, 2014; Wolf, 2014). The computational effort can further be reduced

by using the efficient algorithm proposed in (Benner et al., 2011) for this kind of Sylvester equations. The linear system of equations in (Benner et al., 2011) can be solved by using sparse solvers like (Castagnotto et al., 2017; Davis, 2004; Demmel et al., 1999a,b) to further save the computational cost. If the weights $W_i(s)$ and $W_o(s)$ are large-scale transfer functions, then P_{13} and Q_{14} should also be replaced with their low-rank approximations like P_i and Q_o . In steps 4 and 5, P_{23} , Q_{24} , P_{12} , and Q_{12} solve *sparse-dense* Sylvester equations, which can again be solved by using the solver in (Benner et al., 2011).

5. Numerical Results

In this section, FWHMOR is tested on three numerical examples. The first example is an illustrative one, which is presented to aid convenient repeatability and validation of all the theoretical results of the paper. The second example is a frequency-weighted MOR problem, and the third example is a controller reduction problem. The original high-order models in the last two examples are taken from the benchmark collection for MOR of (Chahlaoui and Van Dooren, 2005). Although the ROM constructed by FWBT is not optimal in any norm, it offers supreme accuracy and is considered a gold standard for the frequency-weighted MOR problem (Ghafoor and Sreeram, 2008). Therefore, we compare the performance of our algorithm with FWBT. Further, we replace P and Q in FWBT with \hat{P} and \hat{Q} , respectively, to perform approximate FWBT, which we refer to as Approximate-FWBT (A-FWBT) wherein \hat{P} and \hat{Q} are generated by FWHMOR.

5.1. Experimental Setup and Hardware:

In all examples, FWHMOR is initialized arbitrarily, and the mirror images of the poles of the initial guess used in FWHMOR are selected as interpolation points. For the multi-input multi-output (MIMO) example, the residues of the initial guess used in FWHMOR are selected as tangential directions in FWITIA. This ensures a fair comparison between FWITIA and FWHMOR, as both algorithms are expected to behave similarly with this selection. The relative change in the poles of the ROM is used as the stopping criterion with a tolerance of 1×10^{-2} . The Lyapunov and Sylvester equations are solved using MATLAB's *'lyap'* command. The experiments are performed using MATLAB 2016 on a computer with a 2GHz i7 processor, 16GB random access memory, and Windows 10 operating system.

5.2. Illustrative Example

Consider a 6th order system with the following state-space realization

$$A = \begin{bmatrix} 0 & 0 & 0 & 1 & 0 & 0 \\ 0 & 0 & 0 & 0 & 1 & 0 \\ 0 & 0 & 0 & 0 & 0 & 1 \\ -5.4545 & 4.5455 & 0 & -0.0545 & 0.0455 & 0 \\ 10 & -21 & 11 & 0.1 & -0.21 & 0.11 \\ 0 & 5.5 & -6.5 & 0 & 0.055 & -0.065 \end{bmatrix},$$

$$B = [0 \ 0 \ 0 \ 0.0909 \ 0.4 \ -0.5]^T, \ C = [2 \ -2 \ 3 \ 0 \ 0 \ 0].$$

Let the input and output frequency weights be the following

$$A_i = \begin{bmatrix} -2 & -4.375 \\ 8 & 0 \end{bmatrix}, B_i = [2 \ 0]^T, C_i = [1 \ 0],$$

$$A_o = \begin{bmatrix} -5 & -9.375 \\ 16 & 0 \end{bmatrix}, B_o = [2 \ 0]^T, C_o = [2.5 \ 0].$$

The initial guess used in FWHMOR is the following

$$\tilde{A}^{(0)} = \begin{bmatrix} 0.0332 & 5.4109 \\ -4.8283 & -0.2998 \end{bmatrix}, \quad \tilde{B}^{(0)} = [-0.0747 \ -0.2958]^T,$$

$$\tilde{C}^{(0)} = [1.0117 \ -0.2599].$$

Both FWHMOR and FWITIA converge in 4 iterations. The reduction subspaces in FWHMOR are the following

$$\tilde{V} = \begin{bmatrix} 0.2132 & -0.0046 \\ -0.9666 & 0.0623 \\ 0.2671 & -0.0341 \\ 0.14 & 0.348 \\ -1.3601 & -1.6698 \\ 0.6732 & 0.5017 \end{bmatrix} \text{ and } \tilde{W} = \begin{bmatrix} 0.4167 & -0.337 \\ -0.7398 & 0.6556 \\ 0.5269 & -0.3808 \\ 0.0139 & 0.2199 \\ -0.0325 & -0.4411 \\ 0.0137 & 0.2622 \end{bmatrix},$$

which construct the following ROM

$$\tilde{A} = \begin{bmatrix} 0.4059 & 1.6956 \\ -15.6668 & -0.6719 \end{bmatrix}, \tilde{B} = [-0.0186 \ -0.2875]^T,$$

$$\tilde{C} = [3.1608 \ -0.2362].$$

The reduction subspaces in FWITIA are the following

$$\tilde{V} = \begin{bmatrix} 0.0086 & 0.1932 \\ -0.063 & -0.9053 \\ 0.0272 & 0.2621 \\ -0.1994 & -0.1223 \\ 0.9381 & -0.0251 \\ -0.2746 & 0.2427 \end{bmatrix} \text{ and } \tilde{W} = \begin{bmatrix} 0.0084 & 0.4674 \\ -0.1161 & -0.827 \\ -0.0698 & 0.5935 \\ -0.4109 & 0.0283 \\ 0.8306 & -0.0621 \\ -0.4857 & 0.0304 \end{bmatrix},$$

which construct the following ROM

$$\tilde{A} = \begin{bmatrix} 1.4570 & 25.1669 \\ -1.1444 & -1.7230 \end{bmatrix}, \tilde{B} = [0.5377 \ -0.0374]^T,$$

$$\tilde{C} = [0.2248 \ 2.9833].$$

One can verify by using MATLAB's command $T = mldivide(V, V1)$ that the reduction subspaces and the ROMs generated by FWITIA and FWHMOR are related to each other with the similarity transformation $T = \begin{bmatrix} 0.0275 & 0.8906 \\ -0.5842 & -0.7104 \end{bmatrix}$. This numerically confirms the results of Subsection 4.2. The deviations in the optimality conditions

(6)-(8) and the interpolation conditions (14) and (15) (which are denoted by \mathcal{F} and \mathcal{G} , respectively) for both ROMs are tabulated in Table 2. It can be noted that the deviations are so small that these ROMs can be considered as local optima for all practical purposes. Moreover, FWITIA and FWHMOR also provide good approximations of P and Q . The \mathcal{H}_2 - and \mathcal{H}_∞ -norms of the weighted error transfer function $E_w(s)$

Table 2.: Deviation in the optimality conditions

Deviation	FWITIA	FWHMOR
$\ X + \tilde{X}\ _2$	2.90×10^{-4}	1.88×10^{-4}
$\ Y D_i D_i^T + \tilde{Y}\ _2$	1.19×10^{-4}	1.06×10^{-4}
$\ D_o^T D_o \tilde{Z} + Z\ _2$	2.26×10^{-5}	1.46×10^{-5}
$\ \mathcal{F}\ _2$	6.96×10^{-4}	6.96×10^{-4}
$\ \mathcal{G}\ _2$	2.13×10^{-5}	2.13×10^{-5}
$\ P_{13} - \tilde{V} P_{23}\ _2$	0.0946	0.0946
$\ Q_{14} + \tilde{W} Q_{24}\ _2$	0.1097	0.1096
$\ P - \tilde{V} \tilde{P} \tilde{V}^T\ _2$	0.0419	0.0419
$\ Q - \tilde{W} \tilde{Q} \tilde{W}^T\ _2$	0.2247	0.2247

are compared with FWBT in Table 3. It can be noted that FWHMOR and A-FWBT provide good approximation.

Table 3.: Weighted Error

Technique	$\ E_w(s)\ _{\mathcal{H}_2}$	$\ E_w(s)\ _{\mathcal{H}_\infty}$
FWBT	0.0080	0.0471
FWITIA	0.0061	0.0471
FWHMOR	0.0061	0.0471
A-FWBT	0.0061	0.0471

5.3. Clamped Beam

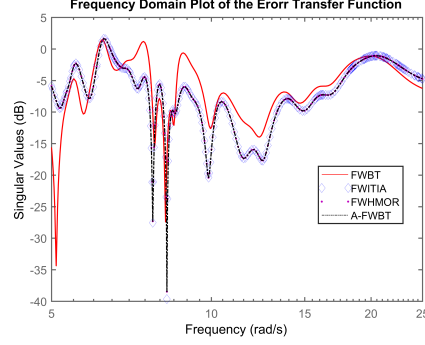
Consider the 348th clamped beam model from the benchmark collection of (Chahlaoui and Van Dooren, 2005). The input weight is a 4th order band-pass filter with the passband $[5, 10]$ rad/sec, which is designed by using MATLAB's command *butter(2, [5, 10], 's')*. The output weight is also a 4th order band-pass filter with the passband $[10, 25]$ rad/sec, which is designed by using MATLAB's command *butter(2, [10, 25], 's')*. A 5th order ROM is obtained by using FWBT, FWITIA, FWHMOR, and A-FWBT. The \mathcal{H}_2 - and \mathcal{H}_∞ -norms of the weighted error transfer function $E_w(s)$ are tabulated in Table 4. It can be seen that FWHMOR and A-FWBT construct accurate ROMs. The singular values of $E(s)$ within $[5, 25]$ rad/sec are plotted in Figure 1. It can be seen that FWHMOR and A-FWBT ensure good accuracy within the desired frequency region.

5.4. International Space Station

Consider the 270th order international space station model from the benchmark collection of (Chahlaoui and Van Dooren, 2005) as the plant $P(s)$. An \mathcal{H}_∞ -controller $K(s)$

Table 4.: Weighted Error

Technique	$\ E_w(s)\ _{\mathcal{H}_2}$	$\ E_w(s)\ _{\mathcal{H}_\infty}$
FWBT	0.3399	0.4418
FWITIA	0.2479	0.2417
FWHMOR	0.2478	0.2408
A-FWBT	0.2478	0.2408

Figure 1.: Singular values of $E(s)$ within $[5, 25]$ rad/sec

is designed using by MATLAB's *ncfsyn* command wherein the loop shaping filter is specified as $\frac{20}{s+1.5}I_{3 \times 3}$. The resulting controller is a 260th order controller, which is reduced to 2nd order controller $\tilde{K}(s)$ based on the closeness of the closed-loop transfer function criterion (Obinata and Anderson, 2012), wherein the input and output weights are specified as

$$W_i(s) = (I + P(s)K(s))^{-1} \text{ and } W_o(s) = (I + P(s)K(s))^{-1}P(s).$$

The \mathcal{H}_2 - and \mathcal{H}_∞ -norms of $E_w(s) = W_o(s)(K(s) - \tilde{K}(s))W_i(s)$ are tabulated in Table 5. It can be noted that FWHMOR and A-FWBT show good accuracy.

Table 5.: Weighted Error

Technique	$\ E_w(s)\ _{\mathcal{H}_2}$	$\ E_w(s)\ _{\mathcal{H}_\infty}$
FWBT	0.1361	4.7385
FWITIA	0.0066	0.0951
FWHMOR	0.0066	0.0950
A-FWBT	0.0066	0.0950

6. Conclusion

We addressed the problem of frequency-weighted \mathcal{H}_2 -optimal MOR within the projection framework. It is shown that although the first-order optimality conditions for

the problem can not be inherently met within the projection framework, the deviation in the optimality conditions decays as the order of the ROM increases. A fixed point iteration algorithm is proposed, which generates a nearly (local) optimal ROM. The oblique projection in the proposed algorithm is computed by solving *sparse-dense* Sylvester equations for which several efficient algorithms exist. The numerical results validate the theory developed in the paper.

Acknowledgment

This work is supported in part by National Natural Science Foundation of China under Grant (No. 61873336, 61873335), in part by the National Key Research and Development Program (No. 2020YFB 1708200), in part by the Foreign Expert Program (No. 20WZ2501100) granted by the Shanghai Science and Technology Commission of Shanghai Municipality (Shanghai Administration of Foreign Experts Affairs), in part by 111 Project (No. D18003) granted by the State Administration of Foreign Experts Affairs, and in part by the Fundamental Research Funds for the Central Universities under Grant (No. FRF-BD-19-002A). M. I. Ahmad is supported by the Higher Education Commission of Pakistan under the National Research Program for Universities Project ID 10176.

References

- Ahmad, M. I., Jaimoukha, I., and Frangos, M. (2010). Krylov subspace restart scheme for solving large-scale Sylvester equations. In *Proceedings of the 2010 American Control Conference*, pages 5726–5731. IEEE.
- Anić, B., Beattie, C., Gugercin, S., and Antoulas, A. C. (2013). Interpolatory weighted- \mathcal{H}_2 model reduction. *Automatica*, 49(5):1275–1280.
- Antoulas, A. C. (2005). *Approximation of large-scale dynamical systems*. SIAM.
- Beattie, C. A. and Gugercin, S. (2014). Model reduction by rational interpolation. *Model Reduction and Algorithms: Theory and Applications*, P. Benner, A. Cohen, M. Ohlberger, and K. Willcox, eds., *Comput. Sci. Engrg*, 15:297–334.
- Benner, P., Cohen, A., Ohlberger, M., and Willcox, K. (2017). *Model reduction and approximation: theory and algorithms*, volume 15. SIAM.
- Benner, P., Köhler, M., and Saak, J. (2011). Sparse-dense Sylvester equations in \mathcal{H}_2 -model order reduction. *mpi magdeburg preprints mpimd/11-11*, 2011.
- Benner, P. and Kürschner, P. (2014). Computing real low-rank solutions of Sylvester equations by the factored ADI method. *Computers & Mathematics with Applications*, 67(9):1656–1672.
- Benner, P., Kürschner, P., and Saak, J. (2016). Frequency-limited balanced truncation with low-rank approximations. *SIAM Journal on Scientific Computing*, 38(1):A471–A499.
- Benner, P., Mehrmann, V., and Sorensen, D. C. (2005). *Dimension reduction of large-scale systems*, volume 45. Springer.
- Breiten, T., Beattie, C., and Gugercin, S. (2015). Near-optimal frequency-weighted interpolatory model reduction. *Systems & Control Letters*, 78:8–18.
- Castagnotto, A., Varona, M. C., Jeschek, L., and Lohmann, B. (2017). SSS & SSSMOR: Analysis and reduction of large-scale dynamic systems in MATLAB. *at-Automatisierungstechnik*, 65(2):134–150.
- Chahlaoui, Y. and Van Dooren, P. (2005). Benchmark examples for model reduction of linear time-invariant dynamical systems. In *Dimension Reduction of Large-Scale Systems*, pages 379–392. Springer.

- Davis, T. A. (2004). Algorithm 832: UMFPACK v4. 3—an unsymmetric-pattern multifrontal method. *ACM Transactions on Mathematical Software (TOMS)*, 30(2):196–199.
- Demmel, J. W., Eisenstat, S. C., Gilbert, J. R., Li, X. S., and Liu, J. W. (1999a). A supernodal approach to sparse partial pivoting. *SIAM Journal on Matrix Analysis and Applications*, 20(3):720–755.
- Demmel, J. W., Gilbert, J. R., and Li, X. S. (1999b). An asynchronous parallel supernodal algorithm for sparse Gaussian elimination. *SIAM Journal on Matrix Analysis and Applications*, 20(4):915–952.
- Diab, M., Liu, W., and Sreeram, V. (2000). Optimal model reduction with a frequency weighted extension. *Dynamics and Control*, 10(3):255–276.
- Enns, D. F. (1984). Model reduction with balanced realizations: An error bound and a frequency weighted generalization. In *The 23rd IEEE conference on decision and control*, pages 127–132. IEEE.
- Ghafoor, A., Sreeram, V., and Treasure, R. (2007). Frequency weighted model reduction technique retaining Hankel singular values. *Asian Journal of Control*, 9(1):50–56.
- Ghafoor, A. and Sreeram, V. (2008). A survey/review of frequency-weighted balanced model reduction techniques. *Journal of Dynamic Systems, Measurement, and Control*, 130(6).
- Gugercin, S., Antoulas, A. C., and Beattie, C. (2008). \mathcal{H}_2 model reduction for large-scale linear dynamical systems. *SIAM journal on matrix analysis and applications*, 30(2):609–638.
- Gugercin, S., Sorensen, D. C., and Antoulas, A. C. (2003). A modified low-rank smith method for large-scale Lyapunov equations. *Numerical Algorithms*, 32(1):27–55.
- Halevi, Y. (1990). Frequency weighted model reduction via optimal projection. In *29th IEEE Conference on Decision and Control*, pages 2906–2911. IEEE.
- Huang, X.-X., Yan, W.-Y., and Teo, K. (2001). A new approach to frequency weighted L_2 optimal model reduction. *International Journal of Control*, 74(12):1239–1246.
- Hurak, Z., Sreeram, V., Wang, G., Van Gestel, T., De Moor, B., Anderson, B., and Van Overschee, P. (2001). Discussion on ‘On frequency weighted balanced truncation: Hankel singular values and error bounds’ by t. van gestel, b. de moor, bdo anderson, and p. van overschee. *European Journal of Control*, 7(6):593–595.
- Kürschner, P. (2018). Balanced truncation model order reduction in limited time intervals for large systems. *Advances in Computational Mathematics*, 44(6):1821–1844.
- Li, J.-R. and White, J. (2002). Low rank solution of Lyapunov equations. *SIAM Journal on Matrix Analysis and Applications*, 24(1):260–280.
- Li, L., Xie, L., Yan, W.-Y., and Soh, Y. C. (1999). \mathcal{H}_2 -optimal reduced-order filtering with frequency weighting. *IEEE Transactions on Circuits and Systems I: Fundamental Theory and Applications*, 46(6):763–767.
- Moore, B. (1981). Principal component analysis in linear systems: Controllability, observability, and model reduction. *IEEE transactions on automatic control*, 26(1):17–32.
- Obinata, G. and Anderson, B. D. (2012). *Model reduction for control system design*. Springer Science & Business Media.
- Panzer, H. K. (2014). *Model order reduction by Krylov subspace methods with global error bounds and automatic choice of parameters*. PhD thesis, Technische Universität München.
- Penzl, T. (1999a). A cyclic low-rank smith method for large sparse Lyapunov equations. *SIAM Journal on Scientific Computing*, 21(4):1401–1418.
- Penzl, T. (1999b). Lyapack: A MATLAB toolbox for large Lyapunov and Riccati equations. *Model Reduction Problems, and Linear-Quadratic Optimal Control Problems, SFB*, 393.
- Petersson, D. (2013). *A nonlinear optimization approach to \mathcal{H}_2 -optimal modeling and control*. PhD thesis, Linköping University.
- Rommes, J. and Martins, N. (2006). Efficient computation of multivariable transfer function dominant poles using subspace acceleration. *IEEE transactions on power systems*, 21(4):1471–1483.
- Saak, J., Mena, H., and Benner, P. (2010). Matrix equation sparse solvers (MESS): a MATLAB toolbox for the solution of sparse large-scale matrix equations. *Chemnitz University of Technology, Germany*.

- Sahlan, S., Ghafoor, A., and Sreeram, V. (2007). Properties of frequency weighted balanced truncation techniques. In *2007 IEEE International Conference on Automation Science and Engineering*, pages 765–770. IEEE.
- Spanos, J., Milman, M., and Mingori, D. (1990). Optimal model reduction and frequency-weighted extension. In *Guidance, Navigation and Control Conference*, page 3345.
- Sreeram, V. (2002). On the properties of frequency weighted balanced truncation techniques. In *Proceedings of the 2002 American Control Conference (IEEE Cat. No. CH37301)*, volume 3, pages 1753–1754. IEEE.
- Sreeram, V. and Sahlan, S. (2012). Improved results on frequency-weighted balanced truncation and error bounds. *International Journal of Robust and Nonlinear Control*, 22(11):1195–1211.
- Van Dooren, P., Gallivan, K. A., and Absil, P.-A. (2008). \mathcal{H}_2 -optimal model reduction of mimo systems. *Applied Mathematics Letters*, 21(12):1267–1273.
- Wang, G., Sreeram, V., and Liu, W. (1999). A new frequency-weighted balanced truncation method and an error bound. *IEEE Transactions on Automatic Control*, 44(9):1734–1737.
- Wolf, T. (2014). \mathcal{H}_2 pseudo-optimal model order reduction. PhD thesis, Technische Universität München.
- Wolf, T., Panzer, H., and Lohmann, B. (2013). Model order reduction by approximate balanced truncation: a unifying framework. *at-Automatisierungstechnik*, 61(8):545–556.
- Yan, W.-Y., Xie, L., and Lam, J. (1997). Convergent algorithms for frequency weighted L_2 model reduction. *Systems & control letters*, 31(1):11–20.
- Zulfiqar, U. and Sreeram, V. (2018). Weighted iterative tangential interpolation algorithms. In *2018 Australian & New Zealand Control Conference (ANZCC)*, pages 380–384. IEEE.
- Zulfiqar, U., Sreeram, V., Ahmad, M. I., and Du, X. (2019). Frequency-weighted \mathcal{H}_2 -pseudo-optimal model order reduction. *arXiv preprint arXiv:1909.06106*, *IMA Journal of Mathematical Control & Information* (In Press).
- Zulfiqar, U., Tariq, W., Li, L., and Liaquat, M. (2017). A passivity-preserving frequency-weighted model order reduction technique. *IEEE Transactions on Circuits and Systems II: Express Briefs*, 64(11):1327–1331.